

Fixation of BiOI/BiOBr/MoS₂ Powders on Fiber Cloths for Photocatalytic Degradation of Ammonia Nitrogen from Aqueous Solution

Yi Wei¹, Peiwei Tang¹, Minfeng Huang¹ & Yongzhang Pan¹

¹School of Environment, Jinan University, Guangzhou, China

Correspondence: Yongzhang Pan, School of Environment, Jinan University, Guangzhou 511443, China. E-mail: tpyz@jnu.edu.cn

Received: March 11, 2020

Accepted: March 29, 2020

Online Published: March 31, 2020

doi:10.5539/ep.v9n1p14

URL: <https://doi.org/10.5539/ep.v9n1p14>

Abstract

A novel photocatalyst powder, BiOI/BiOBr/MoS₂, was synthesized by a simple solvothermal method. X-ray diffraction (XRD), specific surface area and pore size analyses, scanning electron microscopy (SEM), transmission electron microscopy (TEM), and X-ray energy spectrometry (EDS) were utilized to characterize the prepared samples. After evaluating the photocatalytic performance of the catalyst, it was loaded on the glass fiber and carbon fiber by polyvinylidene fluoride (PVDF) and N-methylpyrrolidone, respectively. The photocatalytic activity of the composite was investigated by the degradation of ammonia nitrogen wastewater. The fiber cloth solved the problem of separation of powder from solution after reaction, and the presence of the binder reduces the agglomeration of the nanoparticles in the water. After four times repeated experiments, the degradation of simulate ammonia nitrogen wastewater by loaded glass fiber and loaded carbon fiber are 74.1% and 60.58%. Fixation of BiOI/BiOBr/MoS₂ powders on fiber cloth solve the problem of difficult recovery of powder photocatalytic materials and it can be recycled, which has economic valuable.

Keywords: Bismuth halide complex, BiOI/BiOBr/MoS₂ loaded fiber, ammonia nitrogen wastewater, photocatalytic

1. Introduction

Ammonia is one of the major nitrogen-containing pollutants in wastewater (Lee, Park, & Choi, 2002), Ammonia mainly refers to the combined nitrogen in the form of ammonia ions and free nitrogen in water. The content of NH₃ molecules and NH₄⁺ ions in water mainly depends on the pH value, temperature, salinity and other factors of water. When pH<7, NH₄⁺ ions are the main form of ammonia in water; when pH>11, NH₃ molecules are the main form of ammonia in water (Hedstrom, 2001). NH₃ is a nutrient source that can promote eutrophication and algal growth in natural water (Xiao, Qu, Zhao, Liu, & Wan, 2009), the occurrence of red tide is because of the algae bloom. Excessive amounts of NH₃ in the environment can exert harmful on human health (Yuzawa, Mori, Itoh, & Yoshida, 2012). NH₃ attacks the human respiratory system, skin and eyes, and exposure to high concentration (>300 ppm) may cause death (Netting, 2000; Saha & Deng, 2010). To degrade ammonia nitrogen in wastewater, several chemical and physical methods have been developed and applied. Such as biological denitrification, stripping, breakpoint chlorination and ion exchange (Ahmed & Lan, 2012; Degermenci, Ata, Yildiz, & Chemistry, 2012; Eilbeck, 1984; Ricardo, Carvalho, Velizarov, Crespo, & Reis, 2012). However, most of these methods produced secondary pollution. In order to find an efficient denitrification technology without secondary pollution, researchers began to investigated advanced oxidation processes (AOPs) applicability to the removal of ammonia from water (Bonsen, Schroeter, Jacobs, & Broekaert, 1997; Schmelling & Gray, 1995). Advanced Oxidation Process (AOPs) refers to a series of redox reactions that treat wastewater by generating and utilizing free radicals, such as hydroxyl radicals (Diya'uddeen, Daud, & Aziz, 2011; Fakhru'l-Razi et al., 2009; Ribeiro, Nunes, Pereira, & Silva, 2015; Shahidi, Roy, & Azzouz, 2015; Yu, Han, & He, 2017). The advantage of using AOPs to treat ammonia nitrogen wastewater is that this method is safety and friendly component for the environment.

Photocatalysis is an advanced oxidation technology that coordinates the action of a catalyst under specific light sources to treat wastewater. Akira Fujishima and Kenichi Honda first discovered the phenomenon of light electrolysis of water on semiconductor materials in 1972 (Fujishima, Rao, & Tryk, 2000). The principle of

photocatalytic degradation of ammonia in water is that the redox reactions between the hydroxyl radicals ($\text{HO}\cdot$), superoxide radicals ($\text{O}_2\cdot^-$) generated inorganic nitrogen ions during the photocatalytic process. Photocatalytic oxidation is achieved through hydroxyl substitution reactions, dehydrogenation reactions, and electron transfer processes. When the light intensity is greater than the semiconductor band gap, electrons are excited and electron-hole pairs generated on the catalyst surface. At the same time, the NO_x molecules which adsorbed on the catalyst surface are seized by the electrons and oxidized (Zhao & Lou, 2008). Photocatalytic reduction refers to NO_2^- and NO_3^- in wastewater which are reduced to N_2 through a photocatalytic reaction.

Degradation of ammonia nitrogen wastewater by photocatalytic can be expressed as the following formulas:



Photocatalytic react through semiconductor materials. Semiconductors have a valence band (VB) and an empty conduction band (CB), with a forbidden band between them, so they can be used as a photosensitizer in the photooxidation process (Hoffmann, Martin, Choi, & Bahnemann, 1995). When a semiconductor material is illuminated at or above the bandgap width, the photogenerated holes on the valence band react with H_2O to form hydroxyl radicals and the conduction band electrons react with O_2 in the solution to form superoxide radicals (Yang, Wang, Yang & Yang, 2017; Liang & Li, 2009), which can reduce the ammonia in wastewater. Ternary semiconductor compound bismuth oxyhalide is a new p-type semiconductor, generally expressed as BiOX , ($\text{X}=\text{F}, \text{Cl}, \text{Br}, \text{I}$). Bismuth is a ternary semiconductor compound which has a layered structure formed by overlapping $[\text{Bi}_2\text{O}_2]^{2+}$ layers and double X ion layers (Chang, Zhu, Fu, & Chu, 2013). Due to the relatively loose structure, the morphology of BiOX is usually shown as flakes or nano-flowers (Deng, Chen, Peng, & Tang). The valence band of Bi^{3+} is formed by the hybridization of the 2p orbital of the O atom and the 6s orbital of the Bi atom. The polarization between orbitals weakens the symmetry of the electronic structure and forms a dipole moment that broadens the valence band of the semiconductor, in that case, semiconductor valence band becomes higher, and forbidden band width becomes narrower (Stoltzfus, Woodward, Seshadri, Klepeis, & Bursten, 2007). According to the calculation of density functional theory, the band gaps of BiOF , BiOCl , BiOBr , and BiOI are 3.34, 2.92, 2.65, and 1.75eV, respectively. Compared with TiO_2 , BiOX has a narrow band gap and a high usage of visible light, it is an efficient and economical semiconductor photocatalytic material.

Heterojunction is a crystalline interface formed by two contacting catalysts which have similar band structure. *Lin and Lee* synthesized a $\text{PbO}_2/\text{BiOBr}$ composite by hydrothermal method, and determined its catalytic performance by the degradation efficiency of the crystal violet (CV) under visible light irradiation (Lin et al., 2016). The experimental results show that the reaction rate of the composite material is three times higher than that of PbO_2 and two times higher than that of BiOBr , which indicates that the existence of heterojunctions inhibits photo-generated electron-hole recombination and improves the catalytic efficiency.

One of the major limitations in the application of the photocatalytic process in wastewater is the separation of powder from solution after reaction (Mohammadi, Sharifnia, & Shavisi, 2016). Immobilization of photocatalysts over a support, such as silica, zeolite and polymers have been used to overcome this disadvantage (Ali, Ismail, Najmy, Alhajry, & A-chemistry, 2014; Park, Park, Kim, Choi, & Reviews, 2013; Tseng et al., 2012). *Shi and Cui* studied photocatalytic activity of TiO_2 coated on an activities carbon fiber, the decoloration of methylene blue by TiO_2/ACFs showed a high degradation efficiency (Shi et al., 2012).

In this paper, BiOI , BiOBr and MoS_2 composite particles were prepared by a solvothermal method and the morphology and structure of the samples were characterized. The simulate ammonia wastewater was degraded by composite materials, and the photocatalytic properties of the different samples were compared. To solve a problem where the photocatalytic material could not be recovered in practical applications, a photocatalytic material with a high degradation performance was selected to be coated on fiber cloth, and examined for its degradation efficiency after repeated use.

2. Experimental Section

2.1 Materials

$\text{Bi}(\text{NO}_3)_3 \cdot 5\text{H}_2\text{O}$ (2 mmol) was dissolved in anhydrous ethanol (30 mL) and stirred for 30 min as solution A. KI (1.2 mmol) and cetyltrimethylammonium bromide (1 mmol) (CTAB) were weighed and dispersed in deionized water (30 mL) and stirred for 30 min as solution B. Solution B was slowly added into A and stirred until the liquid turned orange-red. MoS_2 with a mass fraction of 0/0.5/1/2 wt% was added into the turbid liquid, mixed evenly and transferred to a 100-mL reaction kettle, which was then reacted in an oven at 160°C for 24h. After the reaction was completed and the product was cooled, the precipitation was cleaned and dried in an oven at 60°C for 12 h. $\text{BiOI}/\text{BiOBr}/\text{MoS}_2$ composites with different proportions were then obtained.

Glass fiber and carbon cloth were baked in a muffle furnace at 600°C for 3 h as pretreatment. The catalyst powder (50 mg) was uniformly mixed with polyvinylidene fluoride (5 mg) (PVDF), and an appropriate amount of N-methylpyrrolidone was added. The mixture was uniformly loaded on the fiber cloth with a brush after stirring and sonication.

2.2 Characterization

The crystal structure of the photocatalyst was examined by X-ray diffraction (XRD, D2-PHASER), with an X-ray diffractometer using $\text{CuK}\alpha$ ($\lambda=1.5406\text{\AA}$) radiation in the 2θ range of 5-40°. The Brunauer-Emmett-Teller (BET) method was used to calculate the specific area (S_{BET}) based on the adsorption isotherm. The average pore diameter was obtained from the N_2 sorption/desorption isotherm, which was measured on a Quantachrome NOVA 4000e at -196°C. The morphology and surface characteristics of the sample were observed by scanning electron microscopy (SEM, HITACHI TM3030) and transmission electron microscopy (TEM, JEOL-2100F). The synthesis status of the composite was determined by energy dispersive spectroscopy (EDS, JOEL JPS-9030).

2.3 Photocatalysis Experiment

Ammonium chloride (NH_4Cl) was used to simulate ammonia nitrogen wastewater, 30 mg/L, 50 mg/L, 70 mg/L, and 100 mg/L ammonium chloride solutions were configured. At room temperature, catalyst powder (30 mg) was dispersed in simulated wastewater (30 mL) under magnetic stirring. The light source was placed 40 cm above the vessels for the catalytic experiment. Before each light experiment, the catalytic system was stirred in the dark for 30 min to achieve a dynamic adsorption equilibrium. After the catalysis experiment, the supernatant was subjected to a Nessler colorimetric method.

The removal rate is calculated based on the measured nitrogen concentration of the simulated wastewater, and the calculation formula is:

$$\text{removal rate} = \frac{(C_0 - C)}{C_0} \quad (6)$$

Where C represents the initial nitrogen concentration, C_0 represents the testing nitrogen concentration.

2.4 Loaded Fiber Repetitive Experiments

When performing repetitive experiments, a simple shallow pool reaction device was established as the reaction area, and the simulated ammonia nitrogen wastewater was smoothly and evenly pumped into the shallow tank reactor by peristaltic pump. The remainder of the simulated wastewater was stored in a beaker. A 500 W xenon lamp was placed 40 cm above the liquid level to simulate sunlight. Samples were taken from the beaker every 30 min for nitrogen content testing. Four replicate experiments were performed on each fiber, and each result was compared with the degradation results of the first experiment to investigate whether the material was reusable.

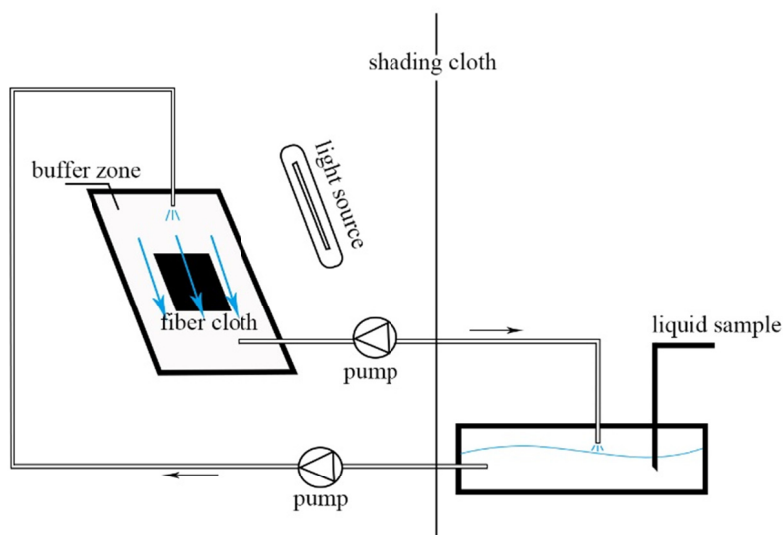


Figure 1. Experimental device

3. Result and Discussion

3.1 Characterization of the Catalyst

XRD patterns in Figure 2 demonstrate that BiOI, BiOBr and composites have obvious diffraction peaks. BiOI exhibits diffraction peaks at 29.7° , 31.9° , 45.8° and 55.4° , which match with the BiOI tetragonal phase (JCPDS10-0445); BiOBr exhibits diffraction peaks at 10.9° , 25.2° , 31.7° , 32.2° , 46.2° and 57.1° , which match with the BiOBr tetragonal phase (JCPDS09-0393). In addition, some impurity peaks show in BiOBr exhibit demonstrate that prepared BiOBr has impurities. BiOI/BiOBr/x wt% MoS₂ composite exhibits sharp diffraction peaks at 30.4° and 32.2° , match with the BiOI and BiOBr's diffraction peaks, proves that the composite has a good crystallization effect. According to the MoS₂ tetragonal phase (JCPDS37-1492), MoS₂ exhibits diffraction peaks at 39.6° and 58.6° , BiOI/BiOBr/x wt% MoS₂ composites show a peak around 39.6° , with increasing x wt%, the peak value at approximately 39.6° increases. However, BiOI/BiOBr/2 wt% MoS₂ still exhibits a blunt tetragonal peak, illustrate that MoS₂ has poor crystallinity in prepared composite material.

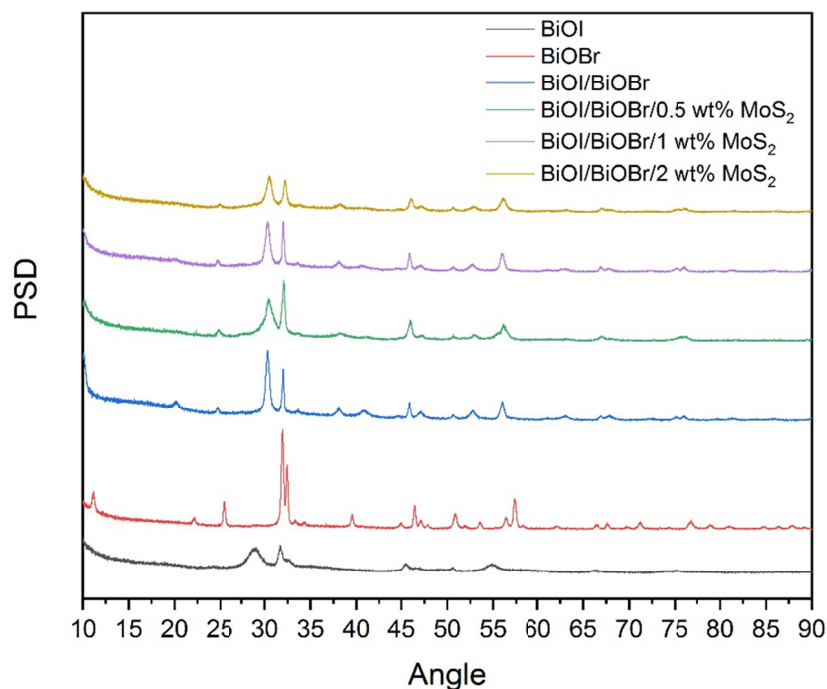


Figure 2. XRD patterns of BiOI, BiOBr, BiOI/BiOBr, BiOI/BiOBr/0.5 wt% MoS₂, BiOI/BiOBr/1 wt% MoS₂ and BiOI/BiOBr/2 wt% MoS₂

The specific surface area of the composite was determined as shown in Table 1. As doped MoS₂ gradually increases, the specific surface area of composite increases, BiOI/BiOBr has an 8.9767 m²/g specific surface area while BiOI/BiOBr/1 wt% MoS₂ has a 13.4604 m²/g specific surface area. Larger specific surface area of the material can provide more active sites for the catalytic reaction, also can improve the catalytic efficiency. However, BiOI/BiOBr/1 wt% MoS₂ has a smaller pore diameter than BiOI/BiOBr/0.5 wt% MoS₂, that may be due to the excess MoS₂ covering the micropores of the BiOI and BiOBr and their composites.

Table 1. BET, pore volume and pore diameter of the composite materials prepared by different samples

I-Br-x%MoS ₂	S _{BET} (m ² /g)	Pore volume (cm ³ /g)	Pore diameter (nm)
x=0	8.9767	0.03920	17.4666
x=0.5	10.1168	0.04785	18.9207
x=1	13.4604	0.05437	16.1567

The SEM image of BiOI/BiOBr/x wt% MoS₂ (x=0, 0.5, 1) showed in Figure 3. Figure 3-a1, b1, c1 magnification is 20k times, Figure 3-a2, b2, c2 magnification is 50k times. A sheet-like stacked structure as shown in the figure was obtained because of using hexadecyltrimethylammonium bromide (CTAB) as the bromine source while preparing the composite. CTAB is an effective cationic surfactant that can condense into cubic, hexagonal, layered structures, also can use for a soft template for continuous growth of crystal grains and plays a decisive role in the microstructure of the material.

MoS₂ is a micro-spherical particle and its diameter is around 1~2μm (Figure 3-d1, d2), compared to Figure 3-a1, a2, the sheet size of the MoS₂ doped composite in Figure 3-b1, b2 and c1, c2 are smaller and there are some irregular crystals on their surface. A particle agglomeration showed in Figure 3-b1, b2 and c1, c2 because of the

doped MoS_2 .

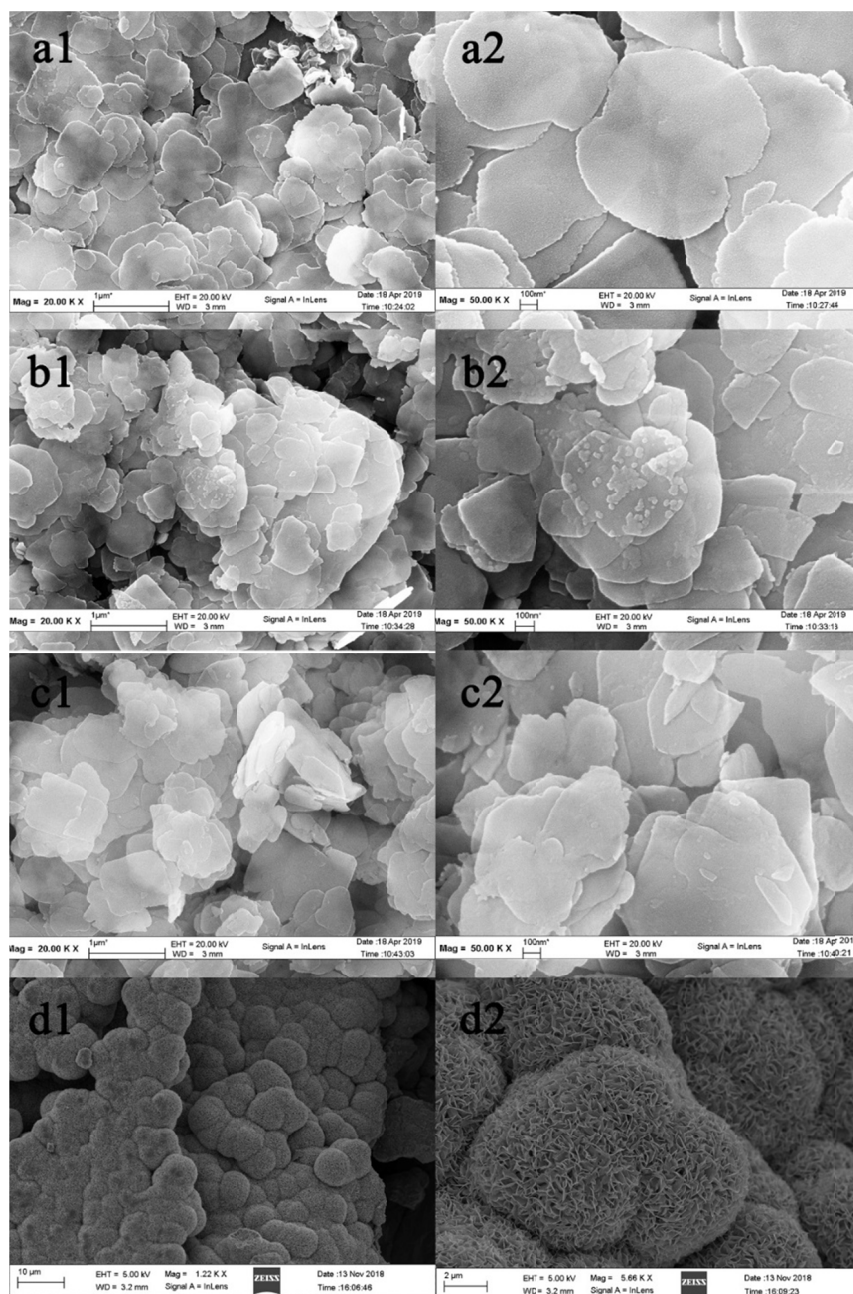


Figure 3. SEM images of (a) BiOI/BiOBr/0 wt% MoS_2 , (b) -0.5 wt% MoS_2 , (c) -1 wt% MoS_2 and (d) MoS_2

TEM photos in Figure 4-a1, b1 and c1 were taken at the edges of BiOI/BiOBr/0 wt% MoS_2 , -0.5 wt% MoS_2 , -1 wt% MoS_2 . An overlapping structure can be seen in the layered material. When the magnification increases to 5 nm, materials with different lattice widths have contact surfaces can be seen in the TEM photos (Figure 4-a2, b2, c2), which proves that heterojunctions were formed during the preparation of the composite. EDS patterns in Figure 4-b3, c3 demonstrated that the presence of Mo and S elements in the composite, with the increasing of x wt% MoS_2 , Mo and S elements content increase.

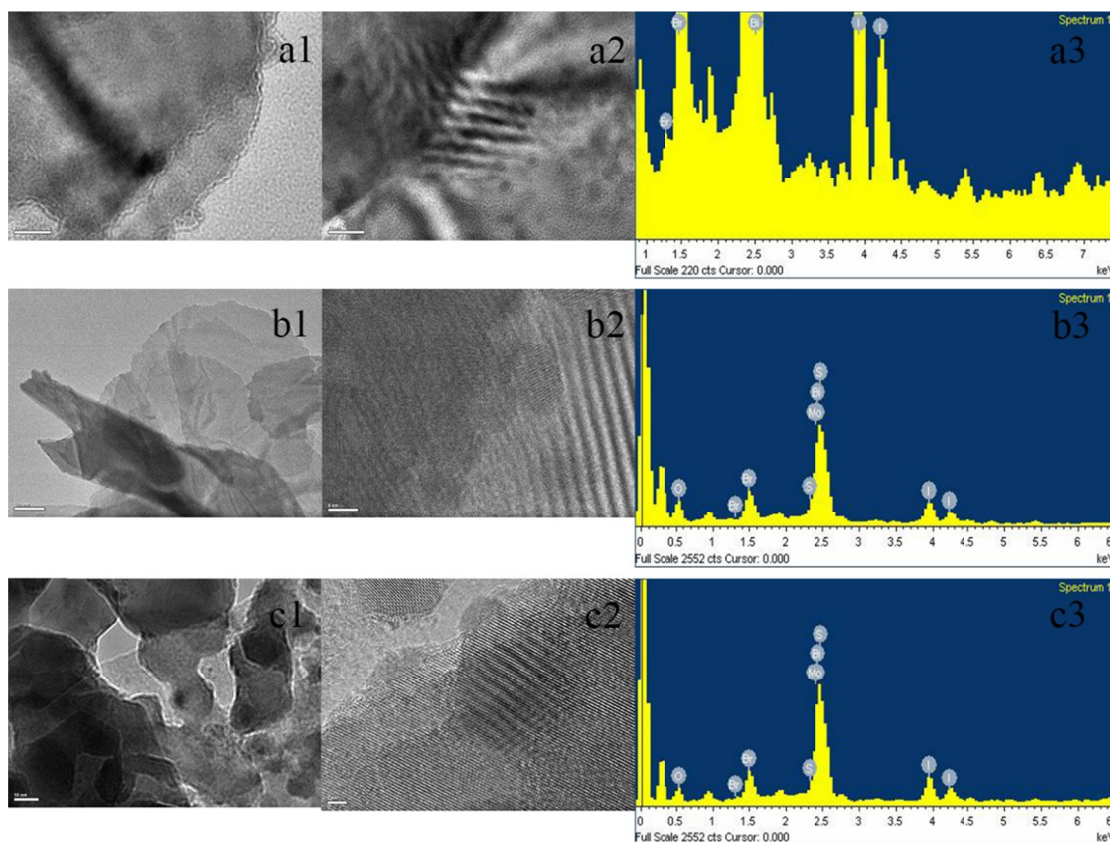


Figure 4. TEM photos and EDS patterns of BiOI/BiOBr/0 wt% MoS₂ (a), -0.5 wt% MoS₂ (b), -1 wt% MoS₂ (c)

3.2 Characterization of Photocatalysis Experiment

In an acidic solution, the main form of N in an ammonia-nitrogen wastewater is NH₄⁺ while in a basic solution, the main form of N is NH₃·H₂O. Due to the lower reaction rate of NH₄⁺ with hydroxyl radicals than NH₃ with hydroxyl radicals, the removal rate in the acidic solution of ammonia wastewater is lower than that in the basic solution (Zhu, Castleberry, Nanny, & Butler, 2005). In addition, in a strong alkaline solution, part of the ammonia may be blown off as the form of NH₃, in that case, although the degradation of ammonia wastewater increase, the photocatalytic efficiency decrease. Therefore, in this paper, the photocatalytic efficiency was investigated under the condition of pH=10 adjusted by NaOH solution.

The photocatalytic of different materials were investigated by the degradation of ammonia nitrogen in the simulate wastewater. The concentrations of nitrogen were 30 mg/L, 50mg/L, 70 mg/L and 100 mg/L. Before the photocatalytic experiment, a 30 min darkroom experiment was performed to reach an adsorption-desorption equilibrium on the surface of the photocatalytic material. After irradiation for 120 min under UV light conditions, the photocatalytic efficiency of the catalyst was observed.

Low initial concentration lead to a low NH₃-N concentration, the active sites on the catalyst surface cannot reach a saturation. At the initial concentration of 30 mg/L ammonia nitrogen wastewater (Figure 5-a), BiOBr has a significant adsorption efficiency and a poor photocatalytic efficiency, the degradation of ammonia by BiOBr is 33.3% while the degradation of ammonia by BiOI/BiOBr is 61.7% after 60 min UV light condition. The doped MoS₂ increased the photocatalytic activity, most ammonia were degraded in 60 minutes, therefore, after 60 minutes reaction, the photocatalytic activity of BiOI/BiOBr is higher than that of BiOI/BiOBr/x wt% MoS₂ (x=0.5, 1, 2). High initial concentration lead to a high NH₃-N concentration, the active sites on the catalyst surface cannot achieve the requirements of the reaction. At the initial concentration of 100 mg/L ammonia nitrogen wastewater (Figure 5-d), after 30 minutes reaction, the photocatalytic activity decrease. At the initial concentration of 50 mg/L and 70 mg/L ammonia nitrogen wastewater (Figure 5-b and c), BiOI/BiOBr/1 wt% MoS₂ shows a high and stable photocatalytic activity, after 90 min reaction, the degradation of ammonia by

BiOI/BiOBr/1 wt% MoS₂ are 78.72% and 77.06% in 50 mg/L and 70 mg/L respectively.

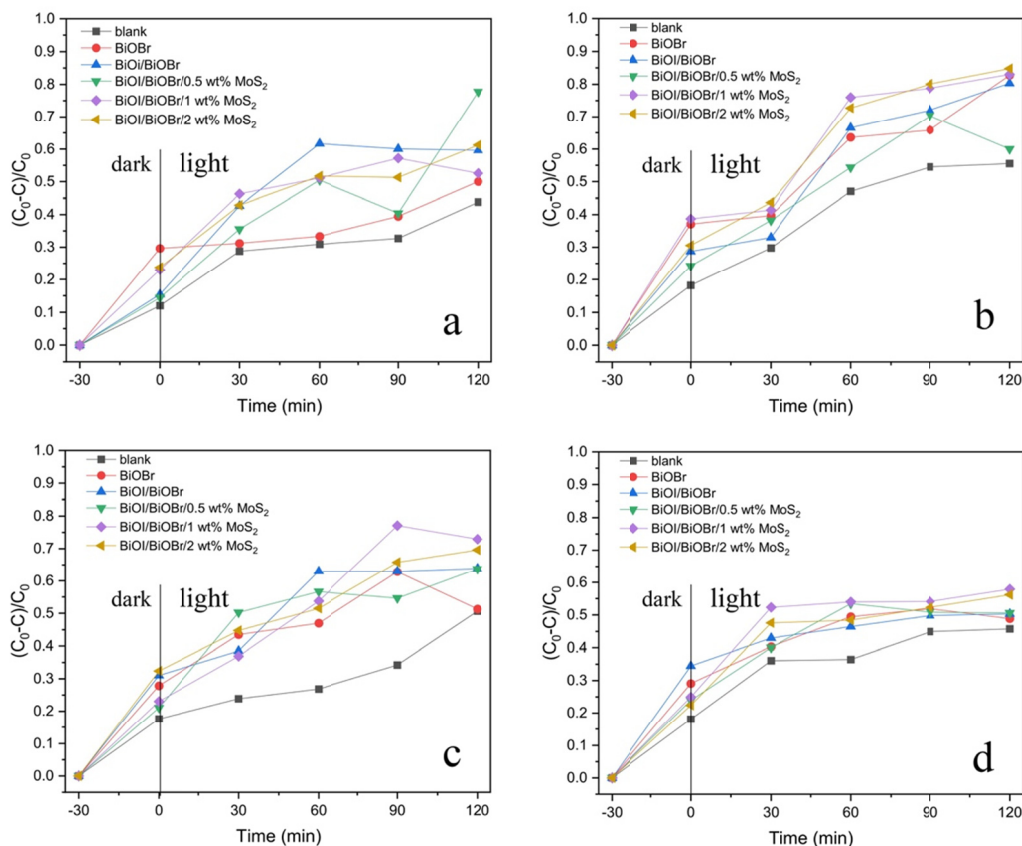


Figure 5. Degradation of simulate ammonia wastewater by photocatalytic material under different initial concentrations: (a) 30 mg/L, (b) 50 mg/L, (c) 70 mg/L and (d) 100 mg/L

3.3 Characterization of the Catalyst in a Visible Light Activity Experiment

The visible light activity of the catalyst was investigated by the degradation of BiOBr and BiOI/BiOBr/1 wt% MoS₂ in the 50 mg/L simulate ammonia nitrogen wastewater, the visible light activity of the catalyst was observed under xenon lamp conditions. As can be seen in Figure 6, after 120 min reaction, the degradation of ammonia by BiOBr under xenon lamp is 63.38% while the degradation of ammonia by BiOI/BiOBr/1 wt% MoS₂ is 80.52%. BiOBr has a wide bandgap, which needs to be excited by high energy wavelength, so the utilization of visible light is low. After the addition of MoS₂ to the catalytic material, the photocatalytic efficiency was significantly increased, because of the electrons excited by the Xe source have a fast transition speed and a slow photogenerated carrier recombination rate.

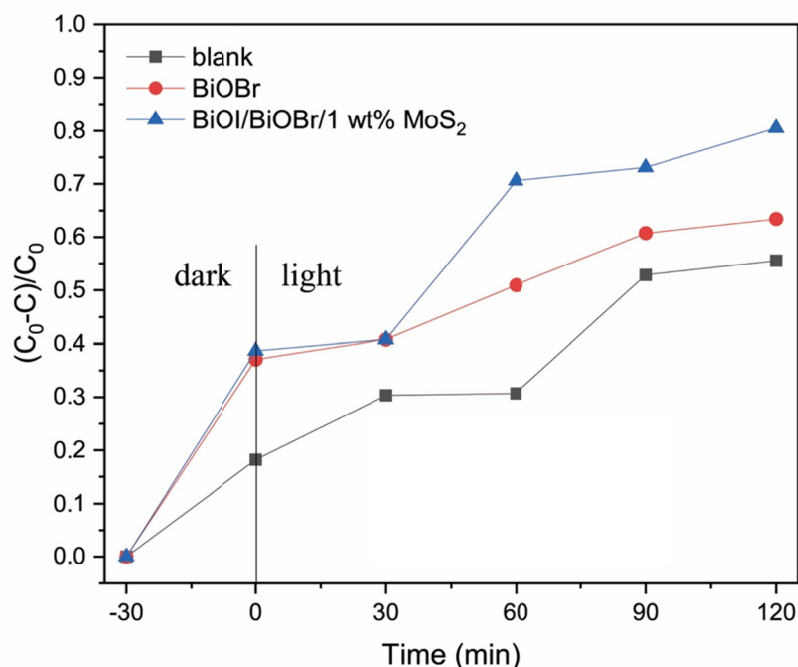


Figure 6. Degradation of simulate ammonia wastewater under xenon lamp condition

3.4 Characterization of the Photocatalytic Products

The purpose of photocatalytic removal ammonia nitrogen wastewater is convert ammonia into nitrogen. *Takeda* investigated that the products of photocatalytic removal ammonia wastewater by TiO_2 and Pt/TiO_2 under 400W xenon lamp condition are nitrate and nitrite (Takeda & Fujiwara, 1996); *Eva-Maria* investigated that the products of photocatalytic removal ammonia wastewater by TiO_2 are related to the reaction pH, when the reaction pH changes from 7.2 to 12.5, the nitrate content in the photocatalytic product increases and then decreases (Bonsen et al., 1997). *Zhu* investigated that oxidation of ammonia into nitrate can be achieved by controlling the oxidation of nitrite (Zhu et al., 2005).

In this paper, we characterization the nitrate content and total nitrogen content after 120 min photocatalytic reaction by $\text{BiOI/BiOBr/1 wt\% MoS}_2$ under UV light condition. The nitrate content is close to 0 and the total nitrogen content is the same as the ammonia nitrogen content, therefore, we speculate that after 120 min photocatalytic reaction by $\text{BiOI/BiOBr/1 wt\% MoS}_2$ under UV light condition, the ammonia is converted into nitrogen.

3.5 Characterization of the Composite Loaded on Fiber Cloth

To further explore the feasibility of the load method, $\text{BiOI/BiOBr/1 wt\% MoS}_2$ was loaded on glass fiber and carbon fiber. The catalytic experiment was under xenon lamp condition for 90 min, after each catalytic experiment was completed, the fibrous material was rinsed with deionized water and then dried in an oven at 60°C . The degradation of 50 mg/L simulate ammonia nitrogen wastewater by loaded-glass fiber and loaded-carbon fiber are shown in Figure 7. After three repeated experiments, the recovery ratio of loaded glass fiber and carbon fiber was 83.84% and 79.94%, after four times repeated, the recovery ratio decrease to 74.1% and 60.58%. Under the conditions of washing rather than activating, the $\text{NH}_3\text{-N}$ molecules adsorbed by the fibers are not completely removed. Therefore, the degradation of ammonia at the second reuse of loaded carbon fiber is higher than that of the first time. Carbon fiber has a poor light transmission, the electrons on $\text{BiOI/BiOBr/1 wt\% MoS}_2$ cannot be fully excited, in consequence, the photocatalytic activity of loaded carbon fiber is lower than that of loaded glass fiber. The photocatalytic properties of the photocatalytic materials were improved after loaded on the glass fiber and carbon fiber, thus $\text{BiOI/BiOBr/1 wt\% MoS}_2$ loaded fiber have a good economic value.

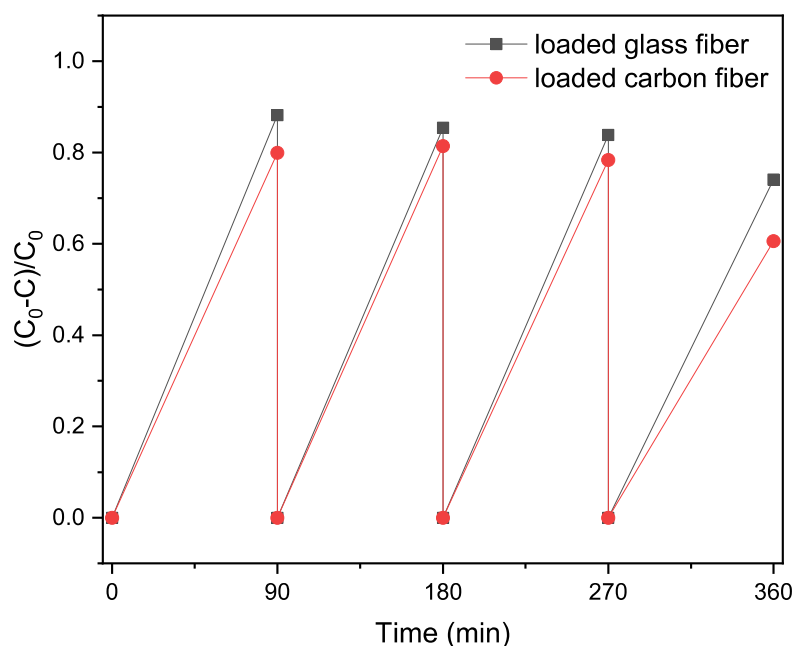


Figure 7. Degradation of simulate ammonia wastewater by loaded glass fiber and loaded carbon fiber

4. Conclusion

Composites were prepared by a solvothermal method. The photocatalytic performance of different catalytic materials was investigated by morphology, structure and their photocatalytic effects on ammonia wastewater. Compared to BiOBr monomer, BiOI/BiOBr/x wt% MoS₂ have higher photocatalytic activity because of the presence of heterojunctions. BiOI/BiOBr/1 wt% MoS₂ composite showed the highest photocatalytic efficiency of degradation of simulate ammonia wastewater. The addition of MoS₂ enhances the nonselective adsorption of materials. However, the excessive doping of MoS₂ may reduce the pore size and decrease the photocatalytic activity of the catalytic. The BiOI/BiOBr/1 wt% MoS₂ material retains a degradation efficiency around 80% when loaded onto a fiber cloth. After four repeated experiments, the recovery ratio of the loaded glass fiber and loaded carbon fiber are 74.1% and 60.58%. The fiber cloth provides more catalytically active sites, and the presence of the binder reduces the agglomeration of the nanoparticles in the water. The loaded fiber cloth prepared in this paper have high photocatalytic activity and can be repeatedly used, which is an economically valuable photocatalytic material.

Acknowledgements

We gratefully acknowledge the skillful and technical supported by Jinan University, School of Environment is acknowledged for providing the XRD patterns, Analytical test center is acknowledged for providing the SEM, TEM and EDS images.

References

- Ahmed, F. N., & Lan, C. Q. (2012). Treatment of landfill leachate using membrane bioreactors: A review. *Desalination*, 287, 41-54. <https://doi.org/10.1016/j.desal.2011.12.012>
- Ali, A. M., Ismail, A. A., Najmy, R., Alhajry, A. J. J. O. P., & A-chemistry, P. (2014). Preparation and characterization of ZnO-SiO₂ thin films as highly efficient photocatalyst, 275, 37-46. <https://doi.org/10.1016/j.jphotochem.2013.11.002>
- Bonsen, E., Schroeter, S., Jacobs, H., & Broekaert, J. C. (1997). Photocatalytic degradation of ammonia with TiO₂ as photocatalyst in the laboratory and under the use of solar radiation. *Chemosphere*, 35(7), 1431-1445. [https://doi.org/10.1016/S0045-6535\(97\)00216-6](https://doi.org/10.1016/S0045-6535(97)00216-6)
- Chang, C., Zhu, L., Fu, Y., & Chu, X. (2013). Highly active Bi/BiOI composite synthesized by one-step reaction

- and its capacity to degrade bisphenol A under simulated solar light irradiation. *Chemical Engineering Journal*, 233, 305-314. <https://doi.org/10.1016/j.cej.2013.08.048>
- Degermenci, N., Ata, O. N., Yildiz, E. J. J. O. I., & Chemistry, E. (2012). Ammonia removal by air stripping in a semi-batch jet loop reactor, *18*(1), 399-404. <https://doi.org/10.1016/j.jiec.2011.11.098>
- Deng, Z., Chen, D., Peng, B., & Tang, F. (n.d.). From Bulk Metal Bi to Two-Dimensional Well-Crystallized BiOX (X = Cl, Br) Micro- and Nanostructures: Synthesis and Characterization. *Crystal Growth & Design*, 8(8), 2995-3003. <https://doi.org/10.1021/cg800116m>
- Diya'uddeen, B. H., Daud, W. M. A. W., & Aziz, A. A. (2011). Treatment technologies for petroleum refinery effluents: A review. *Process safety and environmental protection*, 89(2), 95-105. <https://doi.org/10.1016/j.psep.2010.11.003>
- Eilbeck, W. J. J. W. R. (1984). Redox control in breakpoint chlorination of ammonia and metal ammine complexes, *18*(1), 21-24. [https://doi.org/10.1016/0043-1354\(84\)90043-5](https://doi.org/10.1016/0043-1354(84)90043-5)
- Fakhru'l-Razi, A., Pendashteh, A., Abdullah, L. C., Biak, D. R. A., Madaeni, S. S., & Abidin, Z. Z. (2009). Review of technologies for oil and gas produced water treatment. *Journal of hazardous materials*, 170(2-3), 530-551. <https://doi.org/10.1016/j.jhazmat.2009.05.044>
- Fujishima, A., Rao, T. N., & Tryk, D. A. (2000). Titanium dioxide photocatalysis. *Journal of photochemistry and photobiology C: Photochemistry reviews*, 1(1), 1-21. [https://doi.org/10.1016/S1389-5567\(00\)00002-2](https://doi.org/10.1016/S1389-5567(00)00002-2)
- Hedstrom, A. (2001). Ion exchange of ammonium in zeolites: A literature review. *Journal of Environmental Engineering*, 127(8), 673-681. [https://doi.org/10.1061/\(ASCE\)0733-9372\(2001\)127:8\(673\)](https://doi.org/10.1061/(ASCE)0733-9372(2001)127:8(673))
- Hoffmann, M. R., Martin, S. T., Choi, W., & Bahnemann, D. W. (1995). Environmental applications of semiconductor photocatalysis. *Chemical reviews*, 95(1), 69-96. <https://doi.org/10.1021/cr00033a004>
- Lee, J., Park, H., & Choi, W. (2002). Selective photocatalytic oxidation of NH₃ to N₂ on platinumized TiO₂ in water, *36*(24), 5462. <https://doi.org/10.1021/es025930s>
- Liang, H.-C., & Li, X.-Z. (2009). Visible-induced photocatalytic reactivity of polymer-sensitized titania nanotube films. *Applied Catalysis B: Environmental*, 86(1-2), 8-17. <https://doi.org/10.1016/j.apcatb.2008.07.015>
- Lin, H., Lee, W. W., Huang, S., Chen, L., Yeh, T., Fu, J., & Chen, C. (2016). Controlled hydrothermal synthesis of PbBiO₂Br/BiOBr heterojunction with enhanced visible-driven-light photocatalytic activities. *Journal of Molecular Catalysis A-chemical*, 417, 168-183. <https://doi.org/10.1016/j.molcata.2016.03.021>
- Mohammadi, Z., Sharifnia, S., & Shavisi, Y. (2016). Photocatalytic degradation of aqueous ammonia by using TiO₂ZnO/LECA hybrid photocatalyst. *Materials Chemistry and Physics*, 184, 110-117. <https://doi.org/10.1016/j.matchemphys.2016.09.031>
- Netting, J. (2000). North Carolina reflects on ammonia controls. *Nature*, 406(6799), 928-928. <https://doi.org/10.1038/35023319>
- Park, H., Park, Y., Kim, W., Choi, W. J. J. O. P., & Reviews, P. C.-P. (2013). Surface modification of TiO₂ photocatalyst for environmental applications, *15*, 1-20. <https://doi.org/10.1016/j.jphotochemrev.2012.10.001>
- Ribeiro, A. R., Nunes, O. C., Pereira, M. F., & Silva, A. M. (2015). An overview on the advanced oxidation processes applied for the treatment of water pollutants defined in the recently launched Directive 2013/39/EU. *Environment international*, 75, 33-51. <https://doi.org/10.1016/j.envint.2014.10.027>
- Ricardo, A. R., Carvalho, G., Velizarov, S., Crespo, J. G., & Reis, M. A. (2012). Kinetics of nitrate and perchlorate removal and biofilm stratification in an ion exchange membrane bioreactor. *Water Res*, 46(14), 4556-4568. <https://doi.org/10.1016/j.watres.2012.05.045>
- Saha, D., & Deng, S. (2010). Characteristics of Ammonia Adsorption on Activated Alumina. *Journal of Chemical & Engineering Data*, 55(12), 5587-5593. <https://doi.org/10.1021/jc100405k>
- Schmelling, D. C., & Gray, K. A. (1995). Photocatalytic transformation and mineralization of 2,4,6-trinitrotoluene (TNT) in TiO₂ slurries. *Water Research*, 29(12), 2651-2662. [https://doi.org/10.1016/0043-1354\(95\)00136-9](https://doi.org/10.1016/0043-1354(95)00136-9)
- Shahidi, D., Roy, R., & Azzouz, A. (2015). Advances in catalytic oxidation of organic pollutants—prospects for thorough mineralization by natural clay catalysts. *Applied Catalysis B: Environmental*, 174, 277-292. <https://doi.org/10.1016/j.apcatb.2015.02.042>

- Shi, J., Cui, H., Chen, J., Fu, M., Xu, B., Luo, H., ... Science, I. (2012). TiO₂/activated carbon fibers photocatalyst: Effects of coating procedures on the microstructure, adhesion property, and photocatalytic ability, *388*(1), 201-208. <https://doi.org/10.1016/j.jcis.2012.08.038>
- Stoltzfus, M. W., Woodward, P. M., Seshadri, R., Klepeis, J.-H., & Bursten, B. (2007). Structure and bonding in SnWO₄, PbWO₄, and BiVO₄: lone pairs vs inert pairs. *Inorganic chemistry*, *46*(10), 3839-3850. <https://doi.org/10.1021/ic061157g>
- Takeda, K., & Fujiwara, K. (1996). Characteristics on the determination of dissolved organic nitrogen compounds in natural waters using titanium dioxide and platinumized titanium dioxide mediated photocatalytic degradation. *Water Research*, *30*(2), 323-330. [https://doi.org/10.1016/0043-1354\(95\)00171-9](https://doi.org/10.1016/0043-1354(95)00171-9)
- Tseng, H.-H., Lee, W. W., Wei, M.-C., Huang, B.-S., Hsieh, M.-C., & Cheng, P.-Y. (2012). Synthesis of TiO₂/SBA-15 photocatalyst for the azo dye decolorization through the polyol method. *Chemical Engineering Journal*, *210*, 529-538. <https://doi.org/10.1016/j.cej.2012.09.036>
- Xiao, S., Qu, J., Zhao, X., Liu, H., & Wan, D. (2009). Electrochemical process combined with UV light irradiation for synergistic degradation of ammonia in chloride-containing solutions. *Water Research*, *43*(5), 1432-1440. <https://doi.org/10.1016/j.watres.2008.12.023>
- Yang, C.-X., Wang, X.-N., Yang, S., & Yang, C. (2017). Research on nano-TiO₂ photocatalysis and degradation of dyeing wastewater. *Applied Chemical Industry*, *46*(6), 1185-1189.
- Yu, L., Han, M., & He, F. (2017). A review of treating oily wastewater. *Arabian journal of chemistry*, *10*, S1913-S1922. <https://doi.org/10.1016/j.arabjc.2013.07.020>
- Yuzawa, H., Mori, T., Itoh, H., & Yoshida, H. (2012). Reaction Mechanism of Ammonia Decomposition to Nitrogen and Hydrogen over Metal Loaded Titanium Oxide Photocatalyst. *Journal of Physical Chemistry C*, *116*(6), 4126-4136. <https://doi.org/10.1021/jp209795t>
- Zhao, J.-Y., & Lou, J.-I. (n.d.). Research progress of TiO₂ photocatalytic removal of nitrogen oxides (II). *Chemical Technology Market*, (01), 55-57+61.
- Zhu, X., Castleberry, S. R., Nanny, M. A., & Butler, E. C. (2005). Effects of pH and Catalyst Concentration on Photocatalytic Oxidation of Aqueous Ammonia and Nitrite in Titanium Dioxide Suspensions. *Environmental Science & Technology*, *39*(10), 3784-3791. <https://doi.org/10.1021/es0485715>

Copyrights

Copyright for this article is retained by the author(s), with first publication rights granted to the journal.

This is an open-access article distributed under the terms and conditions of the Creative Commons Attribution license (<http://creativecommons.org/licenses/by/4.0/>).